

Cite this: *Chem. Commun.*, 2012, **48**, 8823–8825

www.rsc.org/chemcomm

COMMUNICATION

Targeted synthesis of a porous borazine-linked covalent organic framework†

Karl T. Jackson, Thomas E. Reich and Hani M. El-Kaderi*

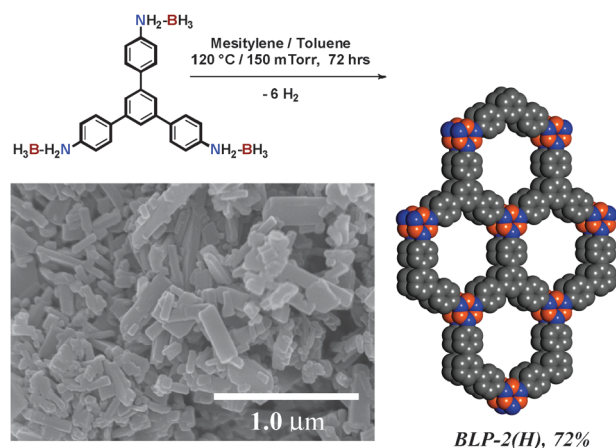
Received 18th May 2012, Accepted 12th July 2012

DOI: 10.1039/c2cc33583b

The first microcrystalline borazine-linked polymer, BLP-2(H), has been synthesized. BLP-2(H) crystallizes into 2D sheets that stack in an eclipsed AA fashion, has high thermal stability ($\sim 420^\circ\text{C}$) and high porosity ($\text{SA}_{\text{BET}} = 1178 \text{ m}^2 \text{ g}^{-1}$) and it can store up to 2.4 wt% of hydrogen at 77 K and 15 bar with isosteric heat of adsorption of 6.8 kJ mol^{-1} .

Covalent-organic frameworks (COFs) are a new class of highly porous microcrystalline materials with promising potential in gas storage, electronics, and catalysis.^{1–4} They can be tailored to possess high porosities, very low densities, and pore metrics that span the microporous and mesoporous ranges. To enhance the porosity and crystallinity of COFs, reversible covalent bond formation such as B–O and C–N under thermodynamic and kinetic controls has been employed that guide the solid-state packing of COFs into predetermined 2D and 3D frameworks. Very recently we have reported on the synthesis of several amorphous borazine-linked polymers (BLPs) and assessed their performance in small gas storage.^{5,6} The thermal decomposition of arylamine–borane or –boron-trihalide adducts in aprotic solvents leads to borazine ring formation which is structurally analogous to the boroxine^{1a,b} and triazine^{1h} building units found in COFs. Borazine has been mainly used for the fabrication of BN-based ceramics or in organic optoelectronics.⁷ However, to date, the use of borazine as a building block for the preparation of porous polymers remains scarce.^{5,6} Polymers linked by B–N bonds are highly sought after, but their preparation remains a great challenge which is very surprising given the isoelectronic nature of the C–C and B–N bonds.⁸ Moreover, crystalline architectures based on B–N bond formation, such as boron nitride (BN) for example, are usually accessible only under high temperature and pressure conditions.⁹

With these considerations in mind we report herein on the targeted synthesis of the first crystalline borazine-linked polymer, BLP-2(H), and investigate its structural aspects, porosity, and performance in hydrogen storage. BLP-2(H) was prepared



Scheme 1 Synthesis of BLP-2(H) and SEM image of as-prepared materials (inset). Space-filling model showing AA stacking; N (blue), B (orange), hydrogen was omitted for clarity.

by the thermal decomposition of 1,3,5-(*p*-aminophenyl)-benzene-borane in a solvent mixture of mesitylene–toluene (1 : 4; vol : vol) at $120^\circ\text{C}/150 \text{ mTorr}$ in a sealed tube for three days which afforded BLP-2(H) as a white microcrystalline powder in good yields (Scheme 1).

BLP-2(H) was isolated under an inert atmosphere, washed with anhydrous dichloromethane then filtered and degassed at $120^\circ\text{C}/1.0 \times 10^{-5} \text{ torr}$ for 16 h prior to characterization and porosity measurements units were investigated by spectral and analytical methods which included FT-IR, solid-state ^{11}B and ^{13}C CP-MAS, and elemental analysis. The formation of the borazine ring was first established by FT-IR studies (Fig. S1, ESI†), which revealed a significant depletion of the amine bands around 3420 cm^{-1} and the formation of characteristic bands consistent with borazine: 2560 cm^{-1} (B–H), 1400 cm^{-1} (B–N stretch).^{5,6} The intensity of the B–H band which appears as a broad intense band at 2400 cm^{-1} in the amine–borane adduct is significantly reduced upon borazine formation. The solid-state ^{11}B and ^{13}C CP-MAS (Fig. S2 and S3, ESI†) further support the formation of the borazine ring and the incorporation of an intact triphenylbenzene moiety into the framework of BLP-2(H). The signal for ^{11}B appears as a broad signal centered about 9.1 ppm which is consistent with tri-coordinate boron and is in sharp contrast to tetra-coordinate boron seen in amine–borane adducts or cycloboranes which

Department of Chemistry, Virginia Commonwealth University, Richmond, VA 23284-2006, USA. E-mail: helkaderi@vcu.edu; Fax: +1 804 828 8599; Tel: +1 804 828 7505

† Electronic supplementary information (ESI) available: Experimental procedures, characterization methods, and gas sorption studies. See DOI: 10.1039/c2cc33583b

usually appear in the negative region (0 to -45 ppm).¹⁰ This signal is also within the range we observed for BLP-1(H) and BLP-12(H), 9–12 ppm.⁶ The morphology and phase purity of BLP-2(H) were investigated by scanning electron microscopy (Scheme 1, inset) which revealed well-defined rectangular prisms of variable size. The crystalline nature of BLP-2(H) was further confirmed by powder X-ray diffraction (PXRD) as depicted in Fig. 1A.

The experimental PXRD pattern was compared against calculated patterns for theoretical models that exhibit eclipsed and staggered conformations of the anticipated 2D sheets following methods reported for 2D COFs.^{1a} Both models where the 2D sheets pack in an eclipsed stacking similar to boron nitride (AA, **bnn**) or in a staggered graphene-like stacking conformation (AB, **gra**) were constructed using *Materials Studio Visualizer* and their geometries were optimized using the Forcite module.¹¹ As shown in Fig. 1, the calculated diffraction pattern of the eclipsed model (Fig. 1B) which in this

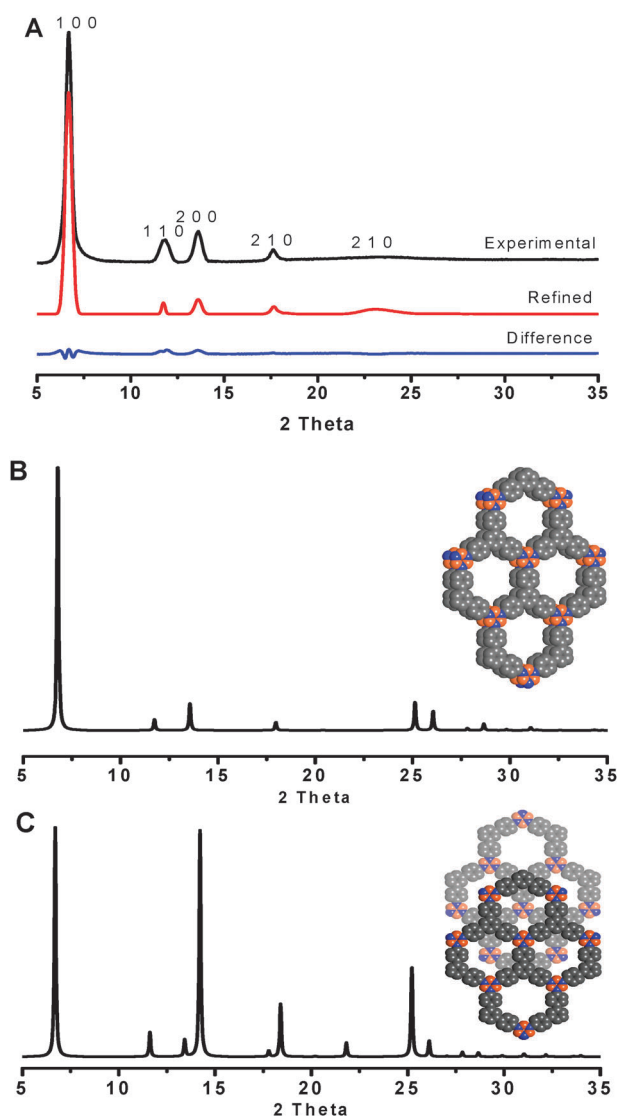


Fig. 1 PXRD pattern of BLP-2(H) with a Cu K α anode (A) with the experimental pattern in black, the Rietveld refined profile in red, and the difference plot in blue. Below are calculated patterns from eclipsed (B) and staggered (C) models.

case has a $P6m_2$ space group is very similar to the experimental PXRD pattern of BLP-2(H) and is in sharp contrast to that of the staggered conformation which would result in a intense signal at $2\theta = 14.22^\circ$ that corresponds to the (101) plane (Fig. 1C). However, the absence of this peak from the experimental PXRD pattern clearly supports the formation of an eclipsed AA packing. The powder XRD pattern of BLP-2(H) was subjected to refinement by the Rietveld¹² method which produced refined PXRD curves with lattice parameters of $a = b = 14.79$ Å and $c = 3.82$ Å. These values agree well with the values of the theoretical eclipsed conformation ($a = b = 15.29$ Å and $c = 3.46$ Å). The spacing between the 2D sheets is slightly larger than what has been found for many chemically or topologically analogous systems including 2D COFs and hexagonal boron nitride (h-BN: 3.33 Å)¹³ but are very similar to that of COF-66 (3.81 Å).^{3a} The noticeably broad (001) peak reflex can arise from poor ordering in the spacing and/or to a small domain size of the 2D layers along this axis. This observation is consistent with 2D COFs in general and especially those featuring functionalized channels wherein the tethered organics seem to perturb the packing of the 2D layers.^{3b} It is also worth mentioning that the formation of 2D COFs based on the tritopic boroxine or triazine building units is not a trivial task. Up to date and to the best of our knowledge, there are only three known 2D COFs featuring boroxine (COF-1,^{1a} PPy-COF^{3c}) and triazine (CTF-1^{1h}) units. One of the difficulties associated with the preparation of 2D COFs featuring these six-membered heterocyclic rings may arise from the lack of sufficient π - π stacking between these units in the solid-state. As a result, COF-1 crystallizes in a staggered AB conformation whereas its triazine analog exists in an eclipsed fashion (AA). The latter packing was also observed for PPy-COF that utilizes pyrene which is well-known for its π - π stacking capability. To investigate the impact of solvents on the formation and crystallinity of BLP-2(H), we have used monoglyme and diglyme under the same conditions reported above for the isolation of crystalline BLP-2(H). The resulting materials from these experimental settings resulted in amorphous polymers that have much lower surface area values ($SA_{BET} = \sim 700$ m² g⁻¹); in addition, the use of only toluene or mesitylene afforded less defined materials as evidenced by SEM and PXRD studies. These results indicate that the formation of crystalline BLP-2(H) is promoted by the use of mesitylene which may have some templating effects^{3d} whereas the use of glymes that dissolve the amine–borane adduct impedes the control over polymerization rates.

To assess the thermal stability and porosity of BLP-2(H), we subjected the as-synthesized material to thermogravimetric analysis under a flow of nitrogen (Fig. S5, ESI†). The TGA trace is typical of covalent porous materials and exhibits ~ 19 wt% loss up to 183 °C presumably due to toluene–mesitylene removal from the pores, then the material remains stable up to ~ 420 °C where decomposition commences. The porous nature of BLP-2(H) was evaluated by argon uptake measurements (Fig. 2A). Prior to porosity measurement, the sample was degassed at 120 °C and 1×10^{-5} torr for 16 h. The Type I argon isotherm is consistent with a permanent microporous material that is characterized by a sharp uptake at low pressure ($P/P_o < 0.1$) whereas the relatively steep Ar uptake

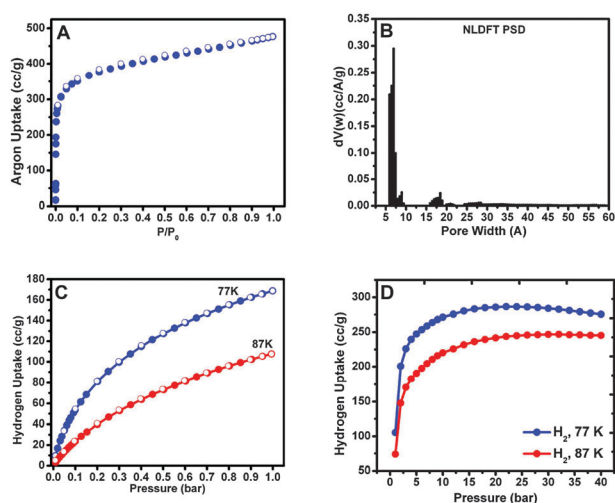


Fig. 2 Argon adsorption isotherm (A), PSD from NLDFT (B), low pressure hydrogen uptake isotherms (C), and high pressure hydrogen uptake isotherms (D); adsorption (filled) and desorption (empty).

beyond $P/P_0 > 0.1$ is most likely due to the filling of meso- and macro-pores present in the sample. A surface area of $1178 \text{ m}^2 \text{ g}^{-1}$ was calculated using the Brunauer–Emmett–Teller (BET) model for P/P_0 between 0.05 and 0.15. Using the Langmuir model ($P/P_0 = 0.05\text{--}0.30$), the surface area value was determined to be $1564 \text{ m}^2 \text{ g}^{-1}$. For comparison, the Langmuir surface area value of BLP-2(H) is similar to the Connolly surface area predicted for the eclipsed model ($1840 \text{ m}^2 \text{ g}^{-1}$) and is much lower than that of the staggered model ($3377 \text{ m}^2 \text{ g}^{-1}$) which further supports the formation of the AA eclipsed stacking. Moreover, the SA_{BET} of BLP-2(H) is higher than those reported for analogous 2D COFs: COF-1 ($711 \text{ m}^2 \text{ g}^{-1}$),² CTF-1 ($791 \text{ m}^2 \text{ g}^{-1}$),^{1h} PPy-COF ($923 \text{ m}^2 \text{ g}^{-1}$)^{3c} as well as amorphous BLPs ($503\text{--}1360 \text{ m}^2 \text{ g}^{-1}$).^{5,6} The pore volume (V_p) was calculated at $P/P_0 = 0.90$ and was found to be $0.59 \text{ cm}^3 \text{ g}^{-1}$ while pore-size distribution from non-local density functional theory (NLDFT) revealed a very narrow PSD centered around 6.4 Å (Fig. 2B).

The higher surface area and narrower PSD observed for BLP-2(H) compared to those of COF-1 and CTF-1 may arise as a result of the deviation of 2D layers from a perfect eclipsed stacking which can introduce a more accessible surface and reduces the dimensions of the pore window.¹⁴ As we have stated earlier, COFs are among the most interesting material for gas storage in general and hydrogen in particular because of its clean aspect and abundance.¹⁵ To investigate the potential of BLP-2(H) in physisorbed hydrogen storage we measured hydrogen storage under cryogenic conditions and a pressure range up to 40 bar (Fig. 2C and D). We have also calculated the isosteric heat of adsorption (Q_{st}) using the virial method from hydrogen isotherms collected at 77 and 87 K.¹⁶ At 1.0 bar and 77 K, the hydrogen uptake for BLP-2(H) is 1.5 wt% (Fig. 2C), which exceeds those of halogenated BLPs and is comparable to similar crystalline organic frameworks: COF-1 (1.28 wt%) and CTF-1 (1.55 wt%). The Q_{st} value was calculated to be 6.8 kJ mol^{-1} at zero coverage (Fig. S11, ESI†). This value is similar to those of previously reported organic

polymers which usually lie somewhere between $5.0\text{--}8.0 \text{ kJ mol}^{-1}$.¹⁷ At a higher pressure range of 1 to 40 bar and 77 K, the H_2 uptake increases gradually with increasing pressure to reach saturation (2.48 wt%) at about 15 bar (Fig. 2D). For comparison, COF-1 stores a much lower amount (1.48 wt%) at higher pressure. This result indicates that a higher surface area would be required to attain substantial amounts of hydrogen as reported for 3D COFs.²

Research supported by the U.S. Department of Energy, Office of Basic Energy Sciences, Division of Materials Sciences and Engineering under Award DE-SC0002576.

Notes and references

- (a) A. P. Côté, A. I. Benin, N. W. Ockwig, M. O’Keeffe, A. J. Matzger and O. M. Yaghi, *Science*, 2005, **310**, 1166; (b) H. M. El-Kaderi, J. R. Hunt, J. L. Mendoza-Cortes, A. P. Côté, R. E. Taylor, M. O’Keeffe and O. M. Yaghi, *Science*, 2007, **316**, 268; (c) A. P. Côté, H. M. El-Kaderi, H. Furukawa, J. R. Hunt and O. M. Yaghi, *J. Am. Chem. Soc.*, 2007, **129**, 12914; (d) R. W. Tilford, W. R. Gemmill, H.-C. zur Loye and J. J. Lavigne, *Chem. Mater.*, 2006, **18**, 5296; (e) J. R. Hunt, C. J. Doonan, J. D. LeVangie, A. P. Côté and O. M. Yaghi, *J. Am. Chem. Soc.*, 2008, **130**, 11872; (f) F. J. Uribe-Romo, J. R. Hunt, H. Furukawa, C. Klöck, M. O’Keeffe and O. M. Yaghi, *J. Am. Chem. Soc.*, 2009, **131**, 4570; (g) F. J. Uribe-Romo, C. J. Doonan, H. Furukawa, K. Oisaki and O. M. Yaghi, *J. Am. Chem. Soc.*, 2011, **133**, 11478; (h) P. Kuhn, M. Antonietti and A. Thomas, *Angew. Chem., Int. Ed.*, 2008, **47**, 3450; (i) M. Dogru, A. Sonner, A. Gavryushin, P. Knochel and T. Bein, *Chem. Commun.*, 2011, **47**, 1707; (j) D. N. Bunck and W. R. Dichtel, *Angew. Chem., Int. Ed.*, 2012, **51**, 1855.
- H. Furukawa and O. M. Yaghi, *J. Am. Chem. Soc.*, 2009, **131**, 8875.
- (a) S. Wan, F. Gándara, A. Asano, H. Furukawa, A. Saeki, S. K. Dey, L. Liao, M. W. Ambrogio, Y. Y. Botros, X. F. Duan, S. Seki, J. F. Stoddart and O. M. Yaghi, *Chem. Mater.*, 2011, **23**, 4094; (b) A. Nagai, Z. Guo, X. Feng, S. Jin, X. Chen, X. Ding and D. Jiang, *Nat. Commun.*, 2011, **2**, 536; (c) S. Wan, J. Guo, J. Kim, H. Ihee and D. Jiang, *Angew. Chem., Int. Ed.*, 2009, **48**, 5439; (d) X. Feng, L. Chen, Y. Dong and D. Jiang, *Chem. Commun.*, 2011, **47**, 1979.
- S.-Y. Ding, J. Gao, Q. Wang, Y. Zhang, W.-G. Song, C.-Y. Su and W. Wang, *J. Am. Chem. Soc.*, 2011, **133**, 19816.
- (a) T. E. Reich, K. T. Jackson, S. Li, P. Jena and H. M. El-Kaderi, *J. Mater. Chem.*, 2011, **21**, 10629; (b) T. E. Reich, S. Behera, K. T. Jackson, P. Jena and H. M. El-Kaderi, *J. Mater. Chem.*, 2012, **22**, 13524.
- K. T. Jackson, M. G. Rabbani, T. E. Reich and H. M. El-Kaderi, *Polym. Chem.*, 2011, **2**, 2775.
- A. Wakamiya, T. Ide and S. Yamaguchi, *J. Am. Chem. Soc.*, 2005, **127**, 14859.
- T. J. Clark, K. Lee and I. Manners, *Chem.–Eur. J.*, 2006, **12**, 8634.
- R. T. Paine and C. K. Narula, *Chem. Rev.*, 1990, **90**, 73.
- (a) C. Gervais, F. Babonneau, J. Maquet, C. Bonhomme, D. Massiot, E. Framery and M. Vaultier, *Magn. Res. Chem.*, 1998, **36**, 407; (b) J. Li, C. Zhang, B. Li, F. Cao and S. Wang, *Eur. J. Inorg. Chem.*, 2010, 1763.
- Accelrys, Inc., *Materials Studio 4.3 V*, Accelrys, Inc., San Diego, CA, 2003.
- H. M. Rietveld, *Acta Crystallogr.*, 1967, **22**, 151152.
- D. Golberg, Y. Bando, Y. Huang, T. Terao, M. Mitone, C. Tang and C. Zhi, *ACS Nano*, 2010, **4**, 2979.
- B. Lukose, A. Kuc and T. Heine, *Chem.–Eur. J.*, 2011, **17**, 2388.
- L. Schlappbach and A. Züttel, *Nature*, 2001, **414**, 353.
- J. L. C. Rowsell and O. M. Yaghi, *J. Am. Chem. Soc.*, 2006, **128**, 1304.
- R. Dawson, A. I. Cooper and D. J. Adams, *Prog. Polym. Sci.*, 2012, **37**, 530.